Design implications of increased live loads on continuous precast, prestressed concrete girder bridges

Antoine N. Gergess and Rajan Sen

- Although American Association of Highway and Transportation Officials (AASHTO) HL93 loads are adopted internationally, British Standards Institution live loads can be as much as 50% higher than HL93 loads and are therefore sometimes used in design in the Middle East.
- This paper investigates the implications of increased live loads on the design of continuous precast, prestressed concrete girders based on service load stress limits.
- The increase in positive moments is economically accommodated by increasing the prestressing force; however, this leads to overstress in the girder end zones over the intermediate supports.
- The authors recommend reducing these stresses by using debonded strands in excess of the 25% limit imposed by AASHTO and making the flanged section solid at the ends to increase the shear capacity.

Precast, prestressed concrete girders are extensively used in the construction of multiple-span, simple-span, and continuous bridges. In the 1960s the concept of making continuous precast, prestressed concrete bridges for live loads was introduced through the use of solid cast-in-place concrete diaphragms[1,2] (**Fig. 1**). The main advantage is that they reduce maintenance costs by eliminating deck joints[3] that are problematic, especially in bridges subjected to heavy truck loading.

Continuity can be introduced by posttensioning as in spliced girders[4] or by erecting the girders as simply supported and subsequently casting the deck and diaphragm (**Fig. 2**). The girders support the weight of the deck and diaphragm as well as construction loads. Continuity is achieved as soon as the deck and diaphragm cure. All subsequent loads, such as live load, superimposed dead loads, and time dependent effects, are supported by the continuous structure.

Structural response

A prestressed concrete girder made continuous is designed for simple support conditions. Continuity introduces negative moments over the supports in the composite sec-

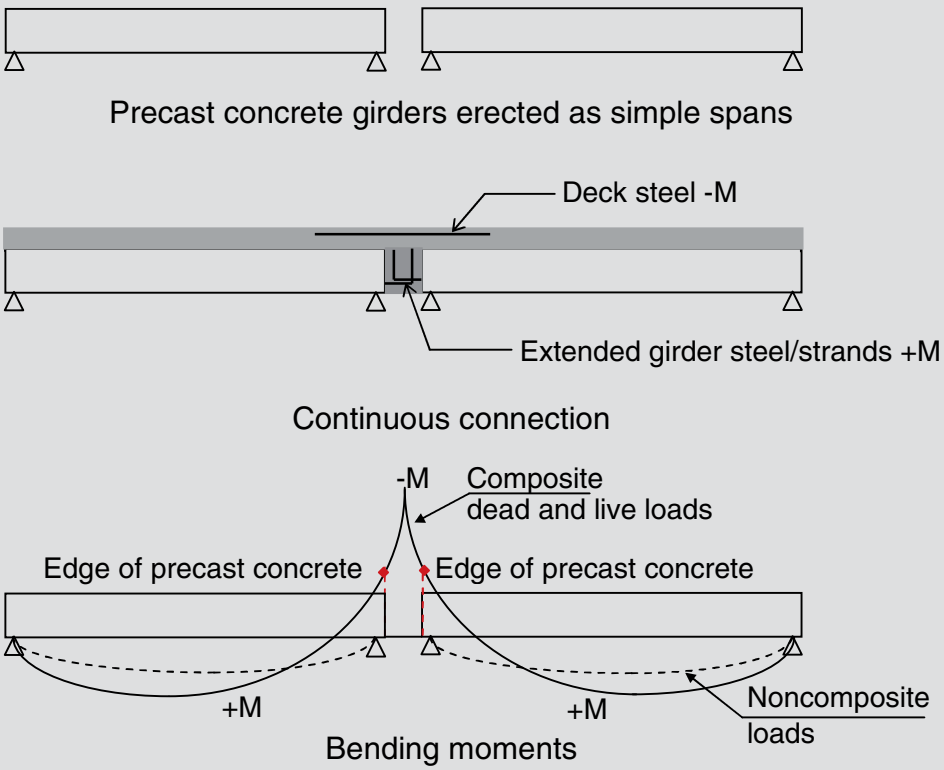

Figure 1. Simple-span precast concrete girders can be made continuous by adding a deck and solid diaphragm and extending girder strands into solid diaphragm and cast-in-place concrete deck. Note: *M* = moment.

tion under live load and superimposed dead load (Fig. 1). Although support moments are reduced by redistribution of positive creep and shrinkage moments in the girders,[5,6] they can still exceed the cracking moment of the reinforced concrete diaphragm and slab, especially if the live loads are increased. Therefore, prestressed girder service load stresses have to be checked in the end zones near the support where the negative moment is highest and prestress is on the compression side. Overstress can occur if design live loads are increased.[7] Current American Association of State Highway and Transportation Officials' *AASHTO LRFD Bridge Design Specifications*[8] allow consideration of special loads, but they normally do not control design in the medium-span range because they are investigated under the smaller strength II limit state. However, outside the United States, higher design live loads, such as those in British Standards Institution's *Steel, Concrete and Composite Bridges—Part 2: Specification for Loads* (BS 5400-2)[9] and *Design Manual for Roads and Bridges*[10] are often specified by relevant authorities[11] for designing structures in ports and heavy industrial areas under AASHTO LRFD specifications service load combinations and can control the service load stress limits.

Overstress (tension or compression) can be reduced by debonding prestressing strands in the girder end-zone regions, but this simple, cost-effective solution is not always used because of restrictions imposed by authorities on the number of strands that can be debonded. For example, AASHTO LRFD specifications stipulate a 25% limit on debonding to ensure that the contribution of the prestress force to shear resistance at the girder's ends is not significantly reduced.[12] This paper proposes an alternative solution to compensate for the decrease in shear capacity due to debonding by providing solid ends in the precast concrete girder in regions where continuity is achieved. New limits on debonding of prestressing strands are consequently recommended.

Objectives

U.S.[8,13] and British[9,14] codes are used worldwide. Authorities in some regions of the Middle East[11] where both codes are permitted require higher live loads than currently stipulated by AASHTO for bridges located near ports and industrial areas that are subjected to frequent heavy truck loads. In such cases, the AASHTO LRFD specifications HL93 live loads are increased 50% to simulate the higher BS 5400-2 live loads. The expectation is that identical bridges designed to either code will result in comparable designs.[15]

Higher live loads result in larger positive moments. Consequently, additional prestressing is required to overcome

During construction

Completed

Aerial view

Figure 2. Construction of a continuous two-span bridge for Shahama-Saadiyat in Abu Dhabi, UAE, designed for American Association of State Highway and Transportation Officials (AASHTO) HL93 live loads increased by 50%. Continuity was achieved by cast-in-place diaphragms and by extending the prestressing strands into the reinforcing steel of the cast-in-place slab and diaphragm. Courtesy of Al-Meraikhi Industrial Complex, UAE.

tension stresses in the positive moment region in the prestressed girder. In this case, methods such as debonding used for reducing overstress in the end zones may not yield workable solutions. This is because in the negative moment region, the prestress force is on the opposite side and may require a greater number of strands to be debonded than the 25% maximum permitted by AASHTO LRFD specifications. As a result, alternative options have to be explored to arrive at a practical solution. This is a nontrivial problem that can require significant design effort because optimal solutions depend on multiple variables, such as span length, girder type, and live load configuration.

This paper first analyzes the effect of increased live load on the design of precast concrete bridges of different lengths made continuous by casting the deck and diaphragm in place. In the study, AASHTO LRFD specifications sections are selected as a representative girder type because of their widespread use in the Middle East and elsewhere. Loads resulting in overstress are then quantified and the applicability of alternative procedures for reducing end-zone overstress for a range of different spans is critically reviewed. Optimal solutions that address cost and practicality based on the recommendations of precast concrete fabricators are finally proposed to control end-zone overstress, and their application is highlighted by an illustrative numerical example.

Background: AASHTO LRFD specifications and BS 5400 live loads

AASHTO LRFD specifications and BS 5400 loads both consist of lane loading and truck loading, but the magnitude and configuration of the loads differ (**Fig. 3**). BS 5400

design live loads designated as lane (HA) and truck (HB) are heavier, and the truck axle configuration is different from the AASHTO LRFD specifications HL93 live load (Fig. 3). Moreover, the BS 5400 loads incorporate the dynamic load allowance (impact) for both lane and truck loads, whereas it only applies for truck and tandem loads in the AASHTO LRFD specifications.

The HA lane load consists of a distributed live load w. For a design span length L less than 50 m (164 ft) and a knife-edge (concentrated) load (KEL) of 120 kN (27 kip):

w (kN/m) = $336(1/L)^{0.67}$ kN/m ($50[1/L]^{0.67}$ kip/ft)

The HB load normally consists of four 300 kN (67 kip) axles spaced at 1.8 m (6 ft) between the first and second axles and the third and fourth axles with a varied spacing of 6 m (20 ft) to 26 m (85 ft) between the middle, second, and third axles (Fig. 3). This results in a gross truck weight of 1200 kN (270 kip), which may be increased 50% to 1800 kN (400 kip). That is, the axle weight is increased from 300 kN (67 kip) to 450 kN (100 kip) if so directed by the relevant authority.

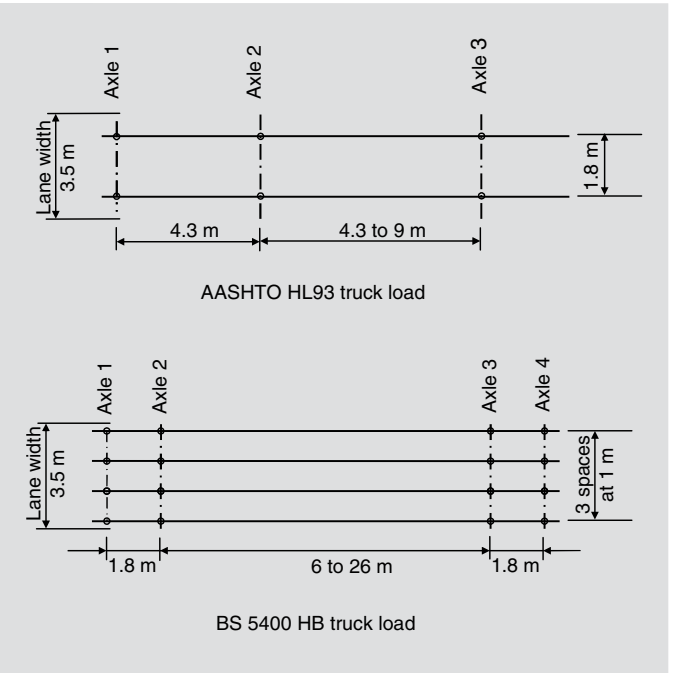

Figure 3. Schematic of axle load distributions. Note: American Association of State Highway and Transportation Officials (AASHTO) axle 1 load = 35 kN (8 kip); AASHTO axles 2 and 3 load = 145 kN (32 kip); British Standards Institution (BSI) axle loads (normal) = 300 kN (67 kip); BSI axle loads (abnormal) = 450 kN (100 kip). 1 m = 3.28 ft.

Application of BS 5400 loading

Because the HB truck loads are significantly higher than HL93, there are differences in how lane loading and truck loading are used in design. Unlike the AASHTO LRFD specifications, BS 5400 specifies that HB loads should be applied in combination with HA loads. That is, for multiple lanes, an HB truck is placed in one lane only while the remaining lanes are loaded with the lighter HA load. If the number of design lanes is greater than or equal to four, the HA loads in the third and subsequent lanes are reduced 40%.

Parametric study

End-zone overstress is the result of complex interactions among a large number of variables. This interaction is best understood through a parametric study that can determine the relationship among the AASHTO LRFD specifications girder type, span length, and live load configuration and identify conditions resulting in the largest overstress.

In the parametric study, the span varied between 12 and 48 m (40 and 160 ft) to reflect the optimal range for available AASHTO standard specification sections (Type II to VI), in addition to a modified Type VI girder called the Type VIM (where M represents modifed), which was specifically developed for increasted live loads[16] (**Fig. 4**). The effects of both AASHTO LRFD specifications HL93 and BS 5400 HA + HB live loadings were considered.

BS 5400 live load moments

The increase in live load moments due to BS 5400 HA + HB loading compared with AASHTO LRFD specifications HL93 loading was determined by plotting the ratio of the induced moments from BS 5400 HA + HB loading to AASHTO HL93 loading (defined as factor β) for various span lengths, girder types, and live load configurations (**Fig. 5**). Results were obtained for positive moments (because they control the prestress force required) using design software, which automatically generates live loads and moment envelopes from which the maximum live load moment can be easily identified.

The design span length of the girder L varied from 12 to 48 m (40 to 160 ft) in 6 m (20 ft) increments, and the appropriate AASHTO LRFD specifications girder cross section (Fig. 4) was used. In the analysis, the separate effects of AASHTO LRFD specifications HL93 and BS 5400 (HA + HB) live loads were determined. HB loading corresponded to the heaviest (1800 kN [400 kip]) and lighter (1200 kN [270 kip]) gross vehicle weights with the middle axles spaced 6 m (20 ft) apart. The AASHTO LRFD specifications HL93 truck and tandem live loads were increased 33% for impact. (BS 5400 loadings include impact.) The analysis was based on simple-span units because maximum positive moments dictate the number of prestressing strands that are used in design.

Figure 5 shows the effects of BS 5400 lane load (HA) and combined lane and truck loads (HA + HB). As expected,

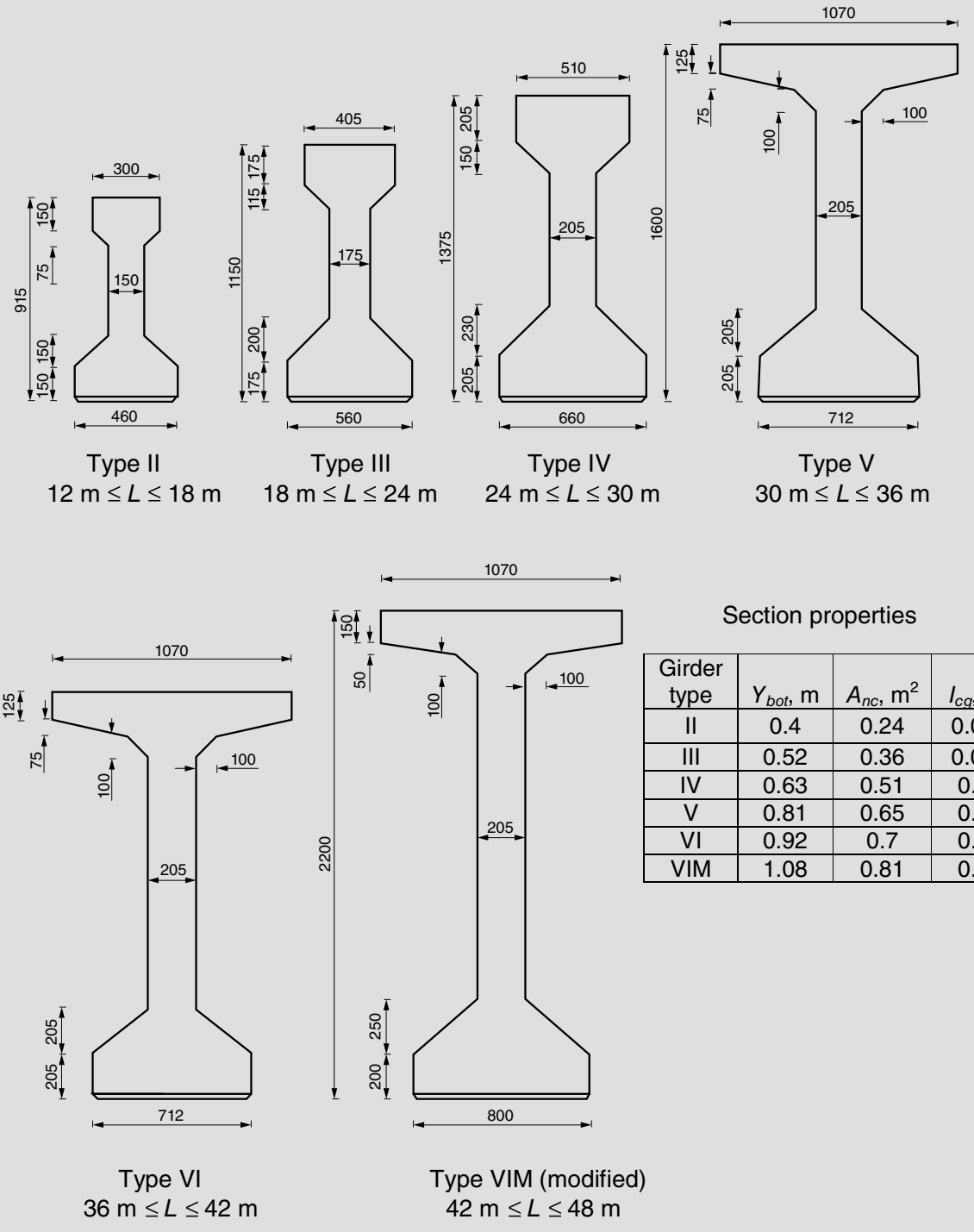

Section properties

Girder type	Y_{bot}, m	A_{nc}, m^2	I_{cg}, m^4
II	0.4	0.24	0.021
III	0.52	0.36	0.053
IV	0.63	0.51	0.11
V	0.81	0.65	0.22
VI	0.92	0.7	0.31
VIM	1.08	0.81	0.52

Figure 4. American Association of State Highway and Transportation Officials Type II to VI girders commonly used for medium spans in addition to a modified Type VI (Type VIM) specifically developed for the Khalifa Port bridges in Abu Dhabi, UAE, adopted in this paper for spans longer than 42 m. Note: A_{nc} = cross-sectional area of prestressed concrete girder; I_{cg} = moment of inertia of precast concrete girder; Y_{bot} = distance from neutral axis of precast concrete girder to the bottom fiber. All dimensions are in millimeters. 1 mm = 0.0394 in.; 1 m = 3.28 ft.

the increase in live load moments was more severe in shorter spans due to the larger concentrated loads and closer spacing of the axles of the truck load. Based on HA lane loading alone, β varied from 1.55 for L of 12 m (40 ft) to 1.18 for L of 48 m (160 ft), indicating higher live load moments than HL93 loading. For the HA + HB combination, β varied from 2.0 for L of 12 m to 1.8 for L of 48 m based on the most critical HB axle load of 450 kN (100 kip).

Design implication on prestress and induced stresses

Figure 5 shows that BS 5400 live load moments exceeded those from the AASHTO LRFD specifications. Consequently, if sections designed using BS 5400 and AASHTO LRFD specifications are to be comparable, the AASHTO LRFD specifications HL93 live load must be increased. In addition, service load combinations and stress limits need to be considered. In a previous study,[15] it was shown that designs based on the BS 5400-4 (HA and HB live loads with the HB axle load set at 300 kN [67 kip] and a service load tensile stress limit of $0.5\sqrt{f_c'}$ MPa [$6\sqrt{f_c'}$ psi], where f_c' is the 28-day concrete cylinder compressive strength) were comparable to AASHTO LRFD specifications if the HL93 live load is increased about 50% and the service load tension stress limit is reduced to zero. This provided a rationale for countries[11] where both codes are permitted and AASHTO LRFD specifications are often adopted.[15]

Increased live load requires a larger prestress force and leads to more prestressing strands if the same girder size and configurations are maintained based on AASHTO LRFD specifications HL93 loads. Given that AASHTO LRFD specifications permit only 25% of the strands to be debonded, end-zone service load stresses under increased live load require careful examination. This can be best understood by reviewing closed form expressions for the end-zone stress variations.

End-zone stresses under normal AASHTO LRFD specifications conditions

The stress state in the end-zone bottom fiber is compressive and is given by Eq. (1). It is based on AASHTO LRFD specifications service I load combination. In this paper a plus (+) sign designates tension and a minus (-) sign designates compression.

$$\text{Bottom fiber: } -F\left[\frac{1}{A_{nc}}+\frac{e}{(S_b)_{nc}}\right]+\frac{M_{ncdl}}{(S_b)_{nc}}+\frac{M_{cdl}}{(S_b)_c}+\frac{M_{LL+I}}{(S_b)_c}\geq(\sigma_{all})_c \quad (1)$$

where

F = effective prestress force

A_{nc} = cross-sectional area of the prestressed concrete girder

e = eccentricity of prestressing tendons

$(S_b)_{nc}$ = bottom fiber noncomposite section modulus

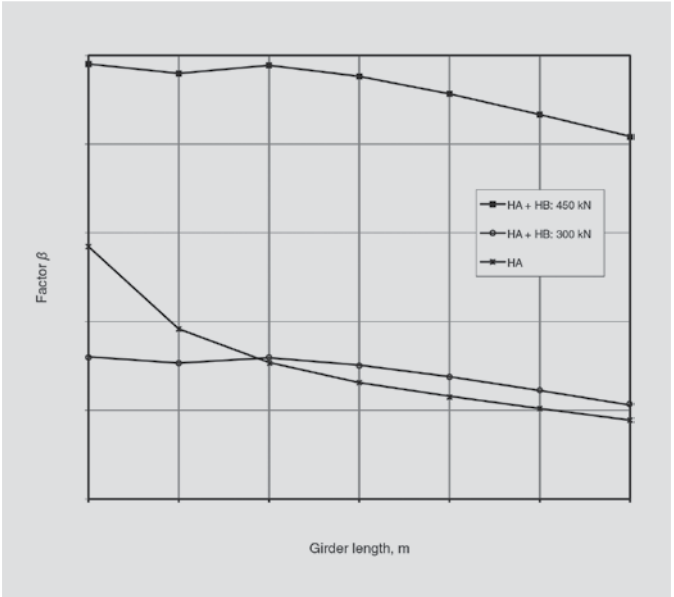

Figure 5. Variation with span length of the ratio of live load moments due to British Standards Institution HA + HB loads to American Association of State Highway and Transportation Officials HL93 loads β under normal environmental conditions. Note: 1 m = 3.28 ft.

M_{ncdl} = noncomposite (positive) dead load moment

M_{cdl} = composite (negative) dead load moment

$(S_b)_c$ = bottom-fiber composite section modulus

M_{LL+I} = moment (negative) due to live load plus impact

$(\sigma_{all})_c$ = allowable service load concrete compressive stress $= 0.6 f_c'$

The noncomposite dead load moment M_{ncdl} is positive because the girder is simply supported for noncomposite dead loads (Fig. 1) and it is usually small. Consequently, the compressive stresses in Eq. (1) induced by the negative moments from superimposed dead loads and live loads add to the compressive stresses due to prestress. Thus, the total compressive stress can exceed the allowable limit $(\sigma_{all})_c$, especially if the live load moment M_{LL+I} is increased by β (Fig. 5).

The corresponding stress state in the top fiber of the precast concrete section in the end zone is tensile. It is given by Eq. (2) following AASHTO LRFD specifications service III load combination:

$$\text{Top fiber: } -F\left[\frac{1}{A_{nc}}-\frac{e}{(S_t)_{nc}}\right]-\frac{M_{ncdl}}{(S_t)_{nc}}-\frac{M_{cdl}}{(S_t)_c}-\frac{0.8M_{LL+I}}{(S_t)_c}\leq(\sigma_{all})_t \quad (2)$$

where

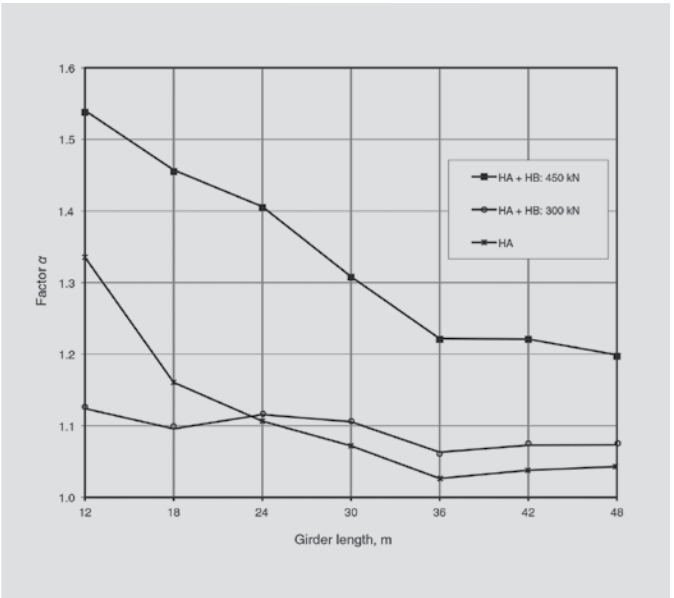

Figure 6. Variation with span length of the factor of increase in effective prestress force (after all losses) due to increased live load α. Note: allowable concrete service load tensile stress in final stage $(\sigma_{all})_t$ equals $0.5\sqrt{f_c'}$ MPa ($6\sqrt{f_c'}$ psi); f_c' = 28-day concrete cylinder compressive strength. 1 m = 3.28 ft.

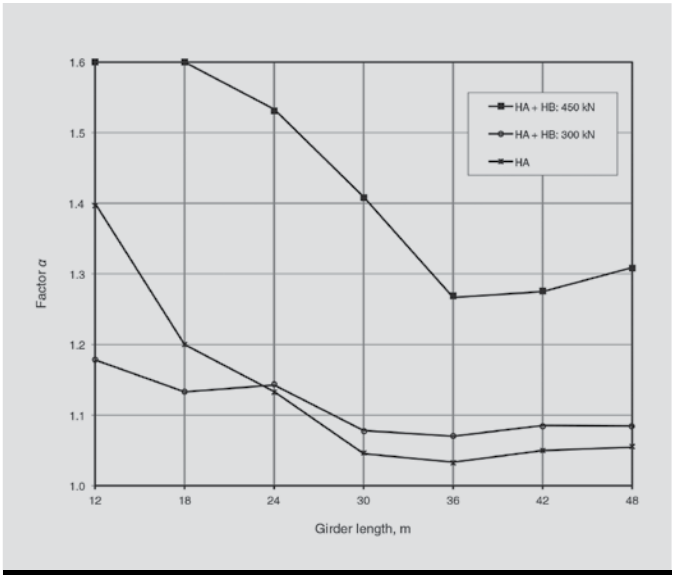

Figure 7. Variation with span length of the factor of increase in jacking prestress force due to increased live load α_1 under normal environmental conditions. Note: allowable concrete service load tensile stress in final stage $(\sigma_{all})_t$ equals $0.5\sqrt{f_c'}$ MPa ($6\sqrt{f_c'}$ psi); f_c' = 28-day concrete cylinder compressive strength. 1 m = 3.28 ft.

$(S_t)_{nc}$ = top-fiber noncomposite section modulus

$(S_t)_c$ = top-fiber composite section modulus

$(\sigma_{all})_t$ = tensile stress limit in the noncompressed top fiber end zones in areas with bonded reinforcement sufficient to resist the tensile force in the concrete computed assuming an uncracked section[8]

$= 0.625\sqrt{f_c'}$ MPa ($7.5\sqrt{f_c'}$ psi)

Because prestress is in the opposite sense over the supports, the most critical location is the transfer point (equal to $60d_b$, d_b being the strand diameter) where the prestress force reaches its full magnitude.[8,12] This is the location where inequalities given by Eq. (1) and (2) must be checked. Because end-zone sections may crack under service-limit state loading, accurate determination of the stress distributions based on strain compatibility and equilibrium of forces may be required.[17]

In actual design, Eq. (1) and (2) should include the effects of creep, shrinkage, and temperature gradient. In the end zones, a positive temperature gradient will add on to the tensile stresses in the top fiber and compression stresses in the bottom fiber.[15] Because these are independent of the live loads and prestress, their effect is not considered in this paper.

Effects of increased live loads on prestressing

Live loads increased by β require a commensurate increase in the prestressing force factor α. It is normally calculated for the maximum induced positive moments. Values of α were determined from a parametric study using design software for the span length and AASHTO LRFD specifications girder ranges considered (Fig. 4).

In the parametric study, the girder spacing and concrete 28-day strength f_c' were not changed (the same configuration was used for a girder subjected to AASHTO LRFD specifications HL93 normal live load and HL93 live load increased by β). The increase in the number of strands (factor α) was determined to control induced service load tensile stresses in the maximum positive moment regions. Recommendations for reducing end-zone overstress are presented later in this paper. The 28-day concrete compressive strength f_c' was 50 MPa (7200 psi), and the concrete compressive strength at release f_{ci}' was about $0.8f_c'$ (required to control large compressive stresses at release near midspan). Higher concrete strengths were not considered because they are difficult to achieve on a consistent basis.[12]

Values of α (**Fig. 6**) are a function of the span length and applied live load. They correspond to the service load tensile stress limit of $0.5\sqrt{f_c'}$ MPa ($6\sqrt{f_c'}$ psi) that is typical for normal environments. Figure 6 shows that for HA lane loading alone, α varied from 1.34 for L of 12 m (40 ft) to 1.04 for L of 48 m (160 ft). For the HA + HB combination, α varied from 1.54 for L of 12 m to 1.2 for L of 48 m (based on HB axle load of 450 kN [100 kip]).

The parametric study was further extended to develop a factor that defines the increase in the number of prestressing strands α_1 (the prestress force before losses) for BS 5400 live loads. Prestress losses were based on the AASHTO LRFD specifications refined method as a function of live load moments (that is, greater live load moments induce greater prestress losses) neglecting elastic gains.

Table 1. Factor of increase in prestress due to reduced service load tensile stress limit

Tension stress limit, MPa	AASHTO HL93	British Standards Institution 5400		
		HA	HA + HB, 300 kN	HA + HB, 450 kN
$(\sigma_{all})_t = 0.25\sqrt{f'_c}$	1.0	1.1	1.08	1.15
$(\sigma_{all})_t = 0$	1.21	1.28	1.27	1.31

Note: AASHTO = American Association of State Highway and Transportation Officials; f'_c = 28-day concrete cylinder compressive strength; $(\sigma_{all})_t$ = allowable concrete service load tensile stress in the final stage

Figure 7 shows the variation in α_1 as a function of the span length and BS 5400 live loadings considered. Factor α_1 varied from 1.6 for L of 12 m (40 ft) to 1.31 for L of 48 m (160 ft) for HA + HB loading with the HB axle load set at 450 kN (100 kip). It varied from 1.4 for L of 12 m to 1.05 for L of 48 m for HA loading only.

As values of α and α_1 were developed for normal environments where $(\sigma_{all})_t$ equals $0.5\sqrt{f'_c}$ MPa ($6\sqrt{f'_c}$ psi), the effect of reducing $(\sigma_{all})_t$ to $0.25\sqrt{f'_c}$ MPa ($3\sqrt{f'_c}$ psi) for an aggressive environment and zero for an extremely aggressive environment was subsequently considered. Based on the parametric study, the increase in the prestress force F due to the reduction in the service load stress limit factor γ was developed. **Table 1** presents values of γ as a function of the live load case. The maximum value of γ was 1.31 when the service load tension stress limit was reduced to zero and the live load was set at HA + HB with the HB axle load equal to 450 kN (100 kip). This led to an increase in prestress of $\alpha\gamma$ that varied from 2.0 for L of 12 m (40 ft) to 1.57 for L of 48 m (160 ft).

Effects of increasing the prestress force on end-zone stresses

The effect of increasing the prestress force on end-zone stresses is illustrated by recasting Eq. (1) and (2) in terms of factors α, β, and γ, which leads to Eq. (3) and (4):

Bottom fiber:

$$-\alpha\gamma F\left(\frac{1}{A_{nc}}+\frac{e}{(S_b)_{nc}}\right)+\frac{M_{ncdl}}{(S_b)_{nc}}+\frac{M_{cdl}}{(S_b)_c}+\beta\frac{M_{LL+I}}{(S_b)_c}\geq(\sigma_{all})_c \quad (3)$$

Top fiber:

$$-\alpha\gamma F\left(\frac{1}{A_{nc}}-\frac{e}{(S_t)_{nc}}\right)-\frac{M_{ncdl}}{(S_t)_{nc}}-\frac{M_{cdl}}{(S_t)_c}-\beta\frac{0.8M_{LL+I}}{(S_t)_c}\leq(\sigma_{all})_t \quad (4)$$

Eq. (3) shows that the increases in the prestress force $\alpha\gamma$ and live load moment β will increase the bottom fiber compressive stress (possible overstress) because its components are all compressive except for the relatively small noncomposite dead load moment M_{ncdl}.

Eq. (4) shows that the top fiber stress components are tensile except for the axial component of the prestress force $(\alpha\gamma F)/A_{nc}$ and the noncomposite dead load moment M_{ncdl} (relatively small), which balances the tensile stress component due to the tendons' eccentricity e. Moreover, according to AASHTO LRFD specifications, the service state tensile stress limit in the top fiber of simple-span precast concrete girders made continuous near interior supports is set equal to the modulus of rupture, that is, $(\sigma_{all})_t$ is $0.625\sqrt{f'_c}$ MPa ($7.5\sqrt{f'_c}$ psi) in Eq. (4). This reduces the possibility of tensile overstress in the end zones but does not necessarily rule them out.

Recommendations for reducing end-zone stresses

The increase in live loads by factor β and the corresponding increase in prestress by factor α can lead to overstress in the end zone (Eq. [3] and [4]). A simple, cost-effective procedure for reducing end-zone stresses is debonding of strands in the girder end zones. AASHTO LRFD specifications limit the number of tendons that can be debonded to 25% of the total number of strands. If end-zone stresses are high, harped strands or straight top strands can be used.

While the latter solutions may be appropriate for moderate increases in live loads, for example, HA and HA + HB loads with an axle load HB of 300 kN (67 kip), they could be restrictive for greater live loads, for example, HA + HB loads with an axle load HB of 450 kN (100 kip), especially if the service-load tensile stress limits are reduced by factor γ in Table 1. In this case, a practical solution for reducing end-zone stresses is to waive the 25% limit on debonding. The limit is considered to be conservative because it is based on the contribution of the prestress force to shear resistance near the girder's ends.[18] This shortfall in shear capacity due to increased debonding is made up by providing solid rectangular ends (**Fig. 8**). Moreover, bond-slip cracking due to debonding, usually found in the thin web section, will be reduced because of the increased width of the web. Harped strands can contribute to reducing

Precast concrete girders during erection

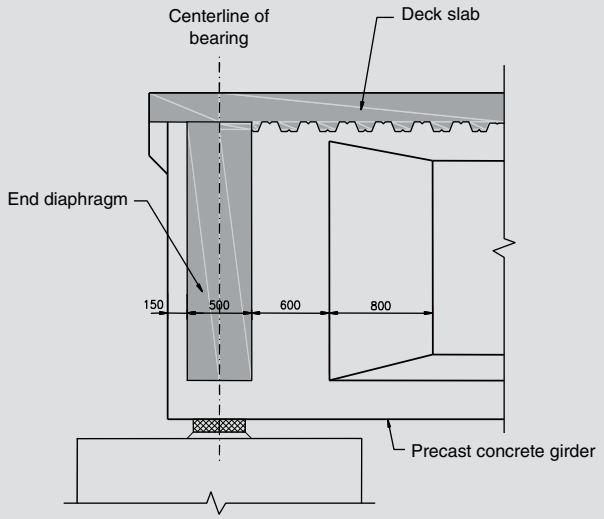

Figure 8. Transition to solid ends for the 39.6 m (130 ft) long Type VIM (modified) precast, prestressed concrete girders that were provided for the new Khalifa Port bridges in Abu Dhabi, UAE. Courtesy of Archirodon Construction, UAE.

end-zone stresses, but they are not a preferred solution for fabricators because of the complexity of placing anchoring devices in regions congested with stirrups and reinforcing steel.

The contribution of solid ends to the shear capacity of precast concrete girders is discussed in detail in the following section. Neither BS 5400-4 nor AASHTO standard specifications impose limits on debonding.

Effect of using solid ends on shear capacity

Under AASHTO LRFD specifications, the shear capacity of a prestressed section is a function of the web thickness b_v and effective shear depth d_v of the precast concrete girder, concrete strength f_c', and compressive strength in concrete due to prestress f_{pc}. From recommendations,[19] the shear capacity of concrete is the lesser of the two resistances for flexure-shear cracking and web-shear cracking (Eq. [5] and [6]). The simplified procedure is used in lieu of the general modified compression field theory because it can better quantify the effect of increasing the web width b_v on the shear capacity.

$$V_{ci} = 0.05\sqrt{f_c'}\,b_v d_v + V_d + \frac{V_i M_{cre}}{M_{max}} \geq 0.17\sqrt{f_c'}\,b_v d_v \qquad (5)$$

where

V_{ci} = shear capacity based on flexure-shear cracking

V_d = shear due to unfactored dead load (MN)

V_i = factored shear force due to externally applied loads (MN)

M_{cre} = cracking moment (MN-m)

M_{max} = factored moment due to externally applied loads (MN-m)

f_c' is in megapascals.

b_v and d_v are in meters.

$$V_{cw} = \left(0.15\sqrt{f_c'} + 0.3f_{pc}\right)b_v d_v + V_p \qquad (6)$$

where

V_{cw} = shear capacity based on web-shear cracking

V_p = vertical component of the prestress force for draped strands (MN)

Over continuous supports, the prestressing steel is on the compression side. This means that prestressing does not increase the cracking moment M_{cre}, and the term $V_i M_{cre}/M_{max}$ in Eq. (5) will be small. As a result, V_{ci} will most likely be controlled by the lower-bound value $0.17\sqrt{f_c'}\,b_v d_v$. Regardless, solid ends will increase V_{ci} because the web thickness b_v will transition to match the flange width (the top flange for Type II to IV girders and the bottom flange for Type V toVIM girders, Fig. 4). If the lower-bound value is assumed, V_{ci} will increase by a factor of 2 for Type II, 2.3 for Type III, 2.5 for Type IV, 3.5 for Types V and VI, and 3.9 for Type VIM (modified) girder.

The contribution due to centroidal prestress $0.3f_{pc}$ in Eq. (6) varies from 300 kPa (44 psi) to 450 kPa (65 psi). These numbers were based on the maximum number of strands that can fit in AASHTO Type II to VIM girders[20] for f_c' of 40, 45, and 50 MPa (5800, 6500, and 7200 psi) using a 75% jacking force, 25% debonding, and 20%

Table 2. Multipliers for the increase in end-zone shear capacity based on solid ends

Girder type	Web thickness, mm	Smaller flange width, mm	Multiplier for V_{ci}	Multiplier for V_{cw}			
				25%	50%	75%	100%
II	150	300 top	2.0	1.9	1.8	1.7	1.5
III	175	400 top	2.3	2.2	2.0	1.9	1.7
IV	200	510 top	2.5	2.3	2.1	2.0	1.8
V	200	712 bottom	3.5	3.0	2.9	2.7	2.6
VI	200	712 bottom	3.5	3.0	2.9	2.7	2.6
VIM	200	800 bottom	3.9	3.3	3.1	3.0	2.8

Note: Percentage values in Table 2 correspond to debonded strands at the solid end. V_{ci} = shear capacity based on flexure-shear cracking; V_{cw} = shear capacity based on web-shear cracking. 1 mm = 0.0394 in.

assumed prestress losses. The component of the concrete strength ($0.15\sqrt{f_c'}$ MPa [$1.8\sqrt{f_c'}$ psi]) in Eq. (6) is calculated as 965 kPa (140 psi) for f_c' of 40 MPa, 1000 kPa (145 psi) for f_c' of 45 MPa, and 1060 kPa (154 psi) for f_c' of 50 MPa. As in Eq. (5), solid ends increase the shear width b_v as well as the cross-sectional area, which will reduce the compressive stress due to prestress f_{pc}. **Table 2** provides the increase in shear strength due to solid ends based on V_{cw} (Eq. [6]) for Type II to Type VIM girders for 25%, 50%, 75%, and 100% debonding in the end zones of solid ends. The increase in shear capacity ranges from 1.5 for Type II to 2.8 for Type VIM even if the centroidal prestress component $0.3f_{pc}$ in Eq. (6) is neglected.

Harped strands also contribute to the shear capacity of the section V_p in Eq. (6). However, the increase in shear capacity is small because of the limited number of strands that can be harped. Solid ends accommodate more stirrups, which results in additional increase in the shear capacity of the end-zone sections. (Their effect is not considered in this paper.)

Effects of using solid ends on end-zone stresses

Solid ends will significantly increase the cross-sectional area of the girder A_{nc} in Eq. (3) and (4). Consequently, the axial component of the stress due to prestress $(\gamma\alpha)F/A_{nc}$ decreases, reducing the compression-induced end-zone stress in the bottom fiber and eliminating possible overstress in compression. On the other hand, the tensile stress in the top fiber (Eq. [4]) will increase, which may make overstress in tension worse. This requires increasing the number of debonded strands above the AASHTO LRFD specifications 25% limit (Table 2).

The increase in the number of debonded strands should make up for the increase in prestress (factors $\alpha\gamma$ in Eq . [3] and [4]). The maximum value of α is 1.55 (Fig. 6) for L of 12 m (40 ft), HA + HB loading where the HB axle load is 450 kN (100 kip) and the maximum value of γ is 1.3 from Table 1 for a service-load tensile stress of zero. This leads to the following calculation:

$$\alpha\gamma = (1.55)(1.3) = 2.0$$

If the AASHTO LRFD specifications 25% limit sets up the basis for debonding in Eq. (1) and (2), then for $\alpha\gamma$ of 2.0, the debonding limit must be increased to

$$\left(100\% - \frac{(100\% - 25\%)}{\alpha\gamma}\right) = 62.5\%$$

This limit decreases as the span length increases. At L of 48 m (160 ft) and α of 1.2, γ is 1.3 (Fig. 6).

$$\alpha\gamma = (1.2)(1.3) = 1.56$$

The percentage debonding required is calculated

$$\left(100\% - \frac{(100\% - 25\%)}{1.56}\right) = 52\%$$

Based on these limits, the increase in shear capacity offsets the reductions due to additional debonding. That is, solid ends increase the shear capacity by a factor that varies from 1.7 for Type II girders to 3.0 for Type VIM girders (based on interpolation between 50% and 75% debonding in Table 2).

Numerical example

The effect of increasing the design live loads on precast, prestressed concrete girders is illustrated by a comprehensive numerical application. The bridge considered for this purpose consists of two 40 m (130 ft) long continuous spans measured from the centerline of end bents to the

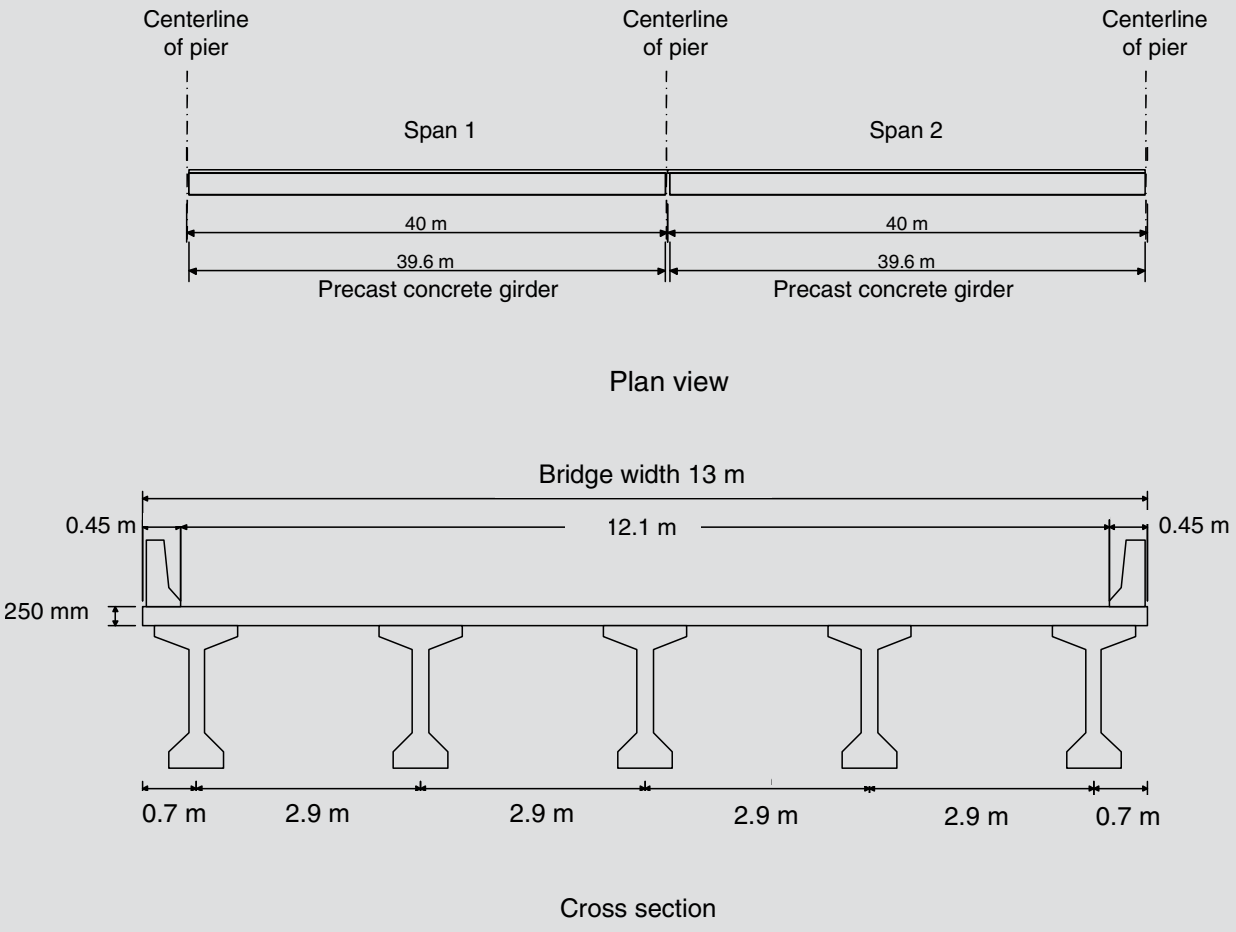

Figure 9. Two-span continuous girders and cross section of the bridge used in the numerical example. Note: 1 mm = 0.0394 in.; 1 m = 3.28 ft.

centerline of intermediate piers (**Fig. 9**). Each span is supported by 39.6 m (130 ft) long AASHTO Type VI precast concrete girders. The design span (between centerlines of bearings) is set at 38.8 m (127 ft). The overall width of the bridge is 13 m (43 ft), comprising two 3.65 m (12.0 ft) wide lanes, a 1.8 m (6 ft) wide inner shoulder, a 3 m wide (10 ft) outer shoulder, and two 0.45 m wide (1.5 ft) barriers (Fig. 9). The girders are first designed to accommodate a normal HL93 live load for a 28-day concrete strength f_c' of 50 MPa (7200 psi) and a service load tension stress limit $(\sigma_{all})_t$ of $0.5\sqrt{f_c'}$, which equals 3500 kPa (510 psi). The effect of reducing this tensile stress to zero is then considered. Finally, the effects of increasing the live load to the BS 5400 HA + HB loading are investigated considering the HB axle load of 300 kN (67 kip) and 450 kN (100 kip) (worst-case scenario) consecutively.

Analysis

The bridge structure supports a 250 mm (10 in.) thick slab to accommodate the heavy axle load of 450 kN (100 kip) of the HB live load, two traffic barriers of 10 kN/m (0.7 kip/ft) each, a 50 mm (2 in.) thick asphalt layer (1.2 kN/m^2 [25 lb/ft^2]), and a utility load of 1 kN/m^2 (20 lb/ft^2). Five AASHTO Type VI girders spaced at 2.9 m (9.5 ft) center to center were used, and the distance from the centerline of the exterior girders to the edge of the slab is 0.7 m (2.3 ft) (Fig. 9). The structural analysis for moments, stresses, prestressing strand distribution, and losses was conducted using design software for a 38.8 m (127 ft) span measured between the centerline of bearings. The live load distribution factors were calculated by design software using AASHTO LRFD specifications equations. Prestress losses were determined from AASHTO LRFD's refined method without considering elastic gains that contribute to reducing losses when superimposed dead loads are applied. The analysis was first conducted for AASHTO LRFD specifications HL93 live loads as follows.

AASHTO LRFD specifications HL93 loading

The prestressing strand layout was determined by design software to resist the maximum positive moments based on a service tensile stress limit of $0.5\sqrt{f_c'}$, which equals 3500 kPa (510 psi). A total of forty-two 15 mm (0.6 in.) diameter strands (40 strands in the bottom flange and 2 in the top flange) were used and 10 strands were debonded, that is, 23.8%, less than the 25% limit.[8]

End-zone stresses were then checked based on the negative moments that develop at the transfer length l_t from the end of the girder.

$l_t = 60d_b = (60)(15) = 900$ mm (36 in.)

Those were calculated using design software as follows:

- Noncomposite dead load: $M_{ncdl} = (172 + 178) =$ 350 kN-m (258 kip-ft) (a positive moment because the girder is laid out as simply supported for noncomposite loads)
- Composite load (barriers + asphalt): $M_{cdl} = -(691 +$ 928) = -1619 kN-m (-1194 kip-ft)
- HL93 live load + impact: $M_{LL+I} = -2800$ kN-m (-2065 kip-ft)

The compressive and tensile stresses that develop in the top and bottom fibers, respectively, were found to be satisfactory. The induced compressive stress was calculated from the design software:

-25.8 MPa (-3700 psi) > $(\sigma_{all})_c = -0.6 f_c^{'}$ = (-0.6)(50) = -30 MPa (-4320 psi)

The tensile stress was calculated from the design software:

4 MPa (600 psi) < $(\sigma_{all})_t = 0.625\sqrt{f_c^{'}}$ = 0.625 $\sqrt{50}$ = 4.42 MPa (630 psi)

The girder was then analyzed for the case where the service load tensile stress limit is set at zero. The increase in the number of strands is designated by a factor γ of 1.21 for HL93 (Table 1). The forty 15 mm (0.6 in.) diameter strands in the bottom flange consequently increased by 1.21 to 49, and the three 15 mm diameter strands in the top flange increased by 1.21 to 3, for a total of 52 strands, 12 (23%) of which were debonded. The compressive and tensile stresses that develop in the top and bottom fibers, respectively, were satisfactory. The induced compressive stress was calculated from the design software:

-28.5 MPa (-4100 psi) > $(\sigma_{all})_c = -0.6 f_c^{'}$ = -(0.6)(50) = -30 MPa (-4320 psi)

The tensile stress was calculated:

3.92 MPa (562 psi) < $(\sigma_{all})_t = 0.625\sqrt{f_c^{'}}$ = 0.625 $\sqrt{50}$ = 4.4 MPa (630 psi)

BS HA + HB loading (HB axle load set 300 kN)

For an HB axle load of 300 kN (67 kip), β is 1.28 for L of 38.8 m (127 ft) from Fig. 5. The corresponding increase in the effective prestress force α was determined to be 1.08 (Fig. 6). The increase in the number of prestressing strands α_1 was determined to be 1.09 (Fig. 7). Consequently, this required the 52 prestressing strands to increase by 1.09 for a total of 57 strands, 53 in the bottom flange and 4 in the top flange (14 strands debonded; that is 24.5%).

The tensile stress in the top fiber is acceptable:

4.1 MPa (590 psi) < $(\sigma_{all})_t = 0.625\sqrt{f_c^{'}}$ = 0.62 $\sqrt{50}$ = 4.4 MPa (630 psi)

However, the compressive stress slightly exceeds the limit:

-30.9 MPa (-4430 psi) < $(\sigma_{all})_c = -0.6 f_c^{'}$ = -(0.6)(50) = -30 MPa (-4320 psi)

This slight overstress can be overcome by increasing the concrete strength to 52 MPa (7500 psi) where

$(\sigma_{all})_c = -0.6 f_c^{'}$ = -(0.6)(52) = -31.2 MPa (-4500 psi) < -30.9 MPa (-4430 psi) OK

BS HA + HB loading (HB axle load set 450 kN)

For an HB axle load of 450 kN (100 kip), β was 1.85 for L of 38.8 m (127 ft) from Fig. 5. The corresponding increase in the effective prestress force α was determined to be 1.22 (Fig. 6). The increase in the number of prestressing strands α_1 was determined to be 1.28 (Fig. 7). Consequently, the required 52 prestressing strands (from the HL 93 live load case and $[\sigma_{all}]_t = 0$) increased by 1.28 for a total of 66 strands, 60 in the bottom flange and 6 in the top flange. An increase in the number of strands necessitated increasing the concrete strength at release from 40 MPa (5800 psi) to 46 MPa (6650 psi).

The tensile stress in the top fiber is acceptable:

3.5 MPa (508 psi) < $(\sigma_{all})_t = 0.625\sqrt{f_c^{'}}$ = 0.625 $\sqrt{50}$ = 4.4 MPa (630 psi)

This tensile stress was also less than the tensile stress of 4.1 MPa (590 psi) for the previous case, where the HB axle load was set at 300 kN (67 kip). This is attributed to the increase in the axial force due to prestress in Eq. (4) $\alpha\gamma F/A_{nc}$ and the decrease in the flexural component in Eq. (4) $\alpha\gamma Fe/(S_t)_{nc}$ due to the reduction in tendon eccentricity e.

However, the compressive stress exceeded the limit:

-37.6 MPa (-5455 psi) < $\sigma_{all})_c = -0.6 f_c^{'}$ = -0.6 × 50 MPa = -30 MPa (-4320 psi)

This overstress is compensated by providing solid ends and increasing the number of debonded strands.

Solid ends For a 712 mm × 1830 mm (28 in. × 72 in.) rectangular beam (based on the smaller bottom flange width

in Fig. 4), the section properties are as follows:

- A_{nc} = 1.34 m^2 (2077 in.^{2})
- $(S_b)_{nc} = (S_t)_{nc}$ = 0.41 m^3 (24,840 in.^{3})
- $(S_b)_c$ = 0.68 m^3 (1100 in.^{3})
- $(S_t)_c$ = 1.48 m^3 (2321 in.^{3}) (based on 2.9 m [9.5 ft] girder spacing)

The effective prestress force $\alpha\gamma F$ was calculated as 5900 kN (1300 kip) based on 11.1% total losses in solid end regions, 75% jacking force, and 32 debonded strands (that is, 48.5% instead of 25%) and e of 0.4 m (1.3 ft).

Calculations are made from Eq. (3) and (4).

Bottom fiber:

$$-\alpha\gamma F\left(\frac{1}{A_{nc}}+\frac{e}{(S_b)_{nc}}\right)+\frac{M_{ncdl}}{(S_b)_{nc}}+\frac{M_{cdl}}{(S_b)_c}+\beta\frac{M_{LL+I}}{(S_b)_c}$$

$$\geq (\sigma_{all})_c$$

$$-5900\left(\frac{1}{1.34}+\frac{0.4}{0.41}\right)+\frac{350}{0.41}+\frac{-1619}{0.68}+(1.85)\left(\frac{-2800}{0.68}\right)$$

$$\geq -0.6(50)$$

-19,300 kN/m^2 = -19.3 MPa (-2800 psi) > -30 MPa (-4351 psi) OK

Top fiber:

$$-\alpha\gamma F\left(\frac{1}{A_{nc}}-\frac{e}{(S_t)_{nc}}\right)-\frac{M_{ncdl}}{(S_t)_{nc}}-\frac{M_{cdl}}{(S_t)_c}-\beta\frac{0.8M_{LL+I}}{(S_t)_c}$$

$$\leq (\sigma_{all})_t$$

$$-5900\left(\frac{1}{1.34}-\frac{0.4}{0.41}\right)-\frac{350}{0.41}-\frac{-1619}{1.48}-(1.85)\left[\frac{(0.8)(-2800)}{1.48}\right]$$

$$\leq (0.625)\left(\sqrt{50}\right)$$

4400 kN/m^2 = 4.4 MPa (638 psi) < 4.42 MPa (641 psi) OK

Stresses were checked at the transfer length of 900 mm (36 in.) from the girder end, which falls within the length of the solid section of 1250 mm (50 in.) that transitions to the I-girder shape over a length of 800 mm (32 in.) in this example (Fig. 8). The debonded length of the strands depends on the magnitude of the negative moments at the transfer length up to the point of inflection (that is usually about 20 % of the precast concrete girder length).

Summary

A 13 m (43 ft) wide bridge deck is supported on five 39.6 m (130 ft) long precast, prestressed concrete AASHTO Type VI concrete girders (Fig. 4) spaced 2.9 m (9.5 ft) apart. The two-span bridge was made continuous at the intermediate pier to support the superimposed dead loads and live loads.

The precast concrete girders in the continuous structure were first analyzed for the normal case of AASHTO LRFD specifications HL93 live load for a service load tensile stress limit of $0.5\sqrt{f_c'}$ MPa ($6\sqrt{f_c'}$ psi) based on positive moments at midspan. This required a total of forty-two 15 mm (0.6 in.) diameter strands (40 in the bottom flange and 2 in the top flange) for a 28-day concrete strength f_c' of 50 MPa (7200 psi) and a release strength f_{ci}' of 40 MPa (5800 psi). Out of 42 strands, 10 (23.8%) were debonded to control the end-zone stresses.

The effect of reducing the service-load tensile stress limit $(\sigma_{all})_t$ from $0.5\sqrt{f_c'}$ equal to 3500 kPa (510 psi) to zero for AASHTO LRFD specifications HL93 live load was then investigated. This required increasing the number of strands from 42 to 52 (49 in the bottom flange and 3 in the top flange) with 12 debonded strands (23%). The girder spacing was maintained at 2.9 m (9.5 ft) and the concrete strength f_c' at 50 MPa (7200 psi).

The effect of increasing the design live loads to BS 5400 HA + HB loads with the HB axle load set at 300 kN (67 kip) and the service load tensile stress limit at zero was then considered. The increase β in live load moments was found to be 1.28 (Fig. 5), and the increase in the number of prestressing strands α_1 was found to be 1.09 (Fig. 7) for a design precast concrete girder length of 39.6 m (130 ft). Consequently, the number of prestressing strands was increased from 52 for AASHTO LRFD specifications HL93 live load to 57 (53 in the bottom flange and 4 in the top flange) with 14 debonded strands (24.5%). The girder spacing and concrete strength were maintained as before.

Finally, the extreme case in which the HB axle load was increased to 450 kN (100 kip) was considered, which increased the live load moments by β of 1.85 (Fig. 5) and the number of prestressing strands by a factor α_1 of 1.28 (Fig. 7) for a service load tensile stress limit of zero. Consequently, the number of prestressing strands required was 66 strands (60 in the bottom flange and 6 in the top flange) compared with 57 strands for the case in which the HB axle load was set at 300 kN (67 kip). To control end-zone stresses, this particular case required providing solid ends in the precast concrete girder sections and increasing the number of debonded strands to 32 (48.5%, exceeding the AASHTO LRFD specifications limit of 25%). The concrete release strength f_{ci}' was also increased from 40 MPa (5800 psi) to 46 MPa (6650 psi) to control compressive

stresses in the midspan region of the girder at release.

The main goal of the numerical example was to maintain the same girder size, spacing, and 28-day concrete strength and make up for the increase in live loads and decrease in the service load stress limits by increasing the number of prestressing strands instead of increasing the number of girders. The savings in cost and time in avoiding the fabrication, transport, and erection of additional girders are more obvious in multiple-span bridge structures where the number of girders can be reduced substantially and can offset the extra cost of the form modifications required for the solid end-zone cross sections.

Conclusion

Precast, prestressed concrete girders made continuous at the supports offer an economical solution to multispan bridge structures by reducing positive moments at midspan and eliminating joints. The girder size, spacing, and prestress force are calculated for the stresses induced by positive moments near midspan. The service load stresses induced by negative moments in the end zones are then checked to comply with AASHTO LRFD specifications criteria. Because these stresses are critical at the girder ends where the negative moment is highest and prestress is on the compression and not the tension side, the AASHTO LRFD specifications' 25% limit on the number of strands that can be debonded can be restrictive, especially if the live loads are increased by the relevant authorities[11] to represent prevailing traffic conditions.

Findings from parametric studies presented show that BS 5400 live loading (HA and HB loads) can induce moments that are double those from AASHTO LRFD specifications HL93 (Fig. 3) normal loads. To maintain the same girder size and configuration, the prestress force should be increased by up to 60% (Fig. 7) for HB truck loading with the axle load set at 450 kN (100 kip) and by an additional 31% (Table 1) if the service load tensile stress is set at zero. This results in overstress in the girder end zone. This overstress can be economically reduced by increasing the 25% AASHTO LRFD specifications debonding limit using solid ends (Fig. 8) to compensate for the shear strength reduction due to debonding in the girder end zones.

Based on the ranges of live loads and service load stress limits set in the parametric study, the worst case scenario, L of 12 m (40 ft), HA + HB loading where the HB axle load is 450 kN (100 kip) necessitates increasing the debonding limit from 25% to 62.5%; this limit reduces to 52% if L is increased to 48 m (160 ft). It was shown that increasing the web thickness to the flange width (the smaller width between the top and bottom flanges) more than doubles the shear capacity and that this shear capacity will still be larger even if all the strands in the end zone are debonded (compared with the 25% limit). It was also shown in the numerical example that the worst live-loading scenario necessitated increasing the debonding limit from 25% to only 48.5%. It is therefore concluded that increasing the web thickness and the number of debonded strands in the end zones can substantially reduce overstress without affecting the shear capacity of the girder. Such a change makes the design provisions consistent with the AASHTO standard specifications and the BS 5400-4 and greatly simplifies design.

References

1. Kaar, P. H., L. B. Kriz, and E. Hognestad. 1960. "Precast-Prestressed Concrete Bridges 1: Pilot Tests of Continuous Girders." *Journal of the PCA Research and Development Laboratories* 2 (2): 21–37. Reprinted as *PCA Bulletin D-34*.

2. Mattock, A. H., and P. H. Kaar. 1960. "Precast-Prestressed Concrete Bridges 3: Further Tests of Continuous Girders." *Journal of the PCA Research and Development Laboratories* 2 (3): 51–78. Reprinted as *PCA Bulletin D-43*.

3. Freyermuth, C. L. 1969. "Design of Continuous Highway Bridges with Precast, Prestressed Concrete Girders." *Journal of the Prestressed Concrete Institute* 14 (2): 14–39. Reprinted as PCA Engineering Bulletin EB014.01E, August 1969.

4. Castrodale, R. W., and C. D. White. 2004. "Extending Span Ranges of Precast, Prestressed Concrete Girders." NCHRP report 517. Washington, DC: TRB (Transportation Research Board of the National Academies).

5. Oesterle, R. G., J. D. Glikin, and S. C. Larson. 1989. "Design of Precast Prestressed Bridge Girders Made Continuous." NCHRP report 322. Washington, DC: TRB.

6. Miller, R. A., R. Castrodale, A. Mirmiran, and M. Hastak. 2004. "Connection of Simple-Span Precast Girders for Continuity." NCHRP report 519. Washington, DC: TRB.

7. Sivakumar, B., and F. Sheikh Ibrahim. 2007. "Enhancement of Bridge Live Loads Using Weigh-in-Motion Data." *Journal of Bridge Structures* 3 (3–4): 193–204.

8. AASHTO (American Association of State Highway and Transportation Officials). 2012. *AASHTO LRFD Bridge Design Specifications.* 6th ed. Washington, DC: AASHTO.

9. BSI (British Standards Institution). 2006. *Steel, Concrete and Composite Bridges—Part 2: Specification for Loads*. BS 5400-2:2006. United Kingdom: BSI.

10. BSI. 2001. "Loads for Highway Bridges." In *Design Manual for Roads and Bridges*, BD37/01, V. 1, section 3, part 14. United Kingdom: BSI.

11. Abu Dhabi Municipality. 2008. Structural Design Requirements for Bridges. Abu Dhabi Municipality Regulations. www.adm.gov.ae.

12. PCI Bridge Design Manual Steering Committee. 2003. *Precast Prestressed Concrete Bridge Design Manual*. MNL-133. 2nd ed. Chicago, IL: PCI.

13. AASHTO. 2007. *Standard Specifications for Highway Bridges*. 17th ed. Washington, DC: AASHTO.

14. BSI. 1990. *Steel, Concrete and Composite Bridge—Part 4: Code of Practice for Design of Concrete Bridges*. BS 5400-4:1990. United Kingdom: BSI.

15. Gergess, A. N., and M. Tepavcevic. 2011. "Implication of Using the British Standards on the Design of Precast, Prestressed Concrete AASHTO Girders." In PCI 57th Annual Convention and National Bridge Conference, Salt Lake City, Utah. October 22–25, 2011. Chicago, IL: PCI.

16. Karapiperis D., G. Lykidis, K. Savvopoulos, K. El-Sayed, and K. Loukakis. 2010. "Combining Effort." *Civil Engineering Magazine* July: pp. 74–85.

17. Wassef, W., C. Smith, C. Clancy, M. Smith. 2003. "Comprehensive Design Example for Prestressed Concrete (PSC) Girder Superstructure Bridge with Commentary." Federal Highway Administration report no. FHWA NHI-04-043, grant no. DTFH61-02-D-63006. Washington, DC: U.S. Government Printing Office.

18. Csagoly, P., H. Bollman, and W. Nickas. 1986. "Cracking Shear Capacity of Prestressed Concrete Beams." In *Official Proceedings: 3rd Annual International Bridge Conference, June 2, 3 & 4, 1986, Hilton Hotel, Pittsburgh, Pennsylvania, U.S.A*. Pittsburgh, PA: Engineers' Society of Western Pennsylvania.

19. Hawkins, N. M., D. A. Kuchma, R. F. Mast, M. L. Marsh, and K. H. Reineck. 2005. "Simplified Shear Design of Structural Concrete Members." NCHRP report 549. Washington, DC: Transportation Research Board.

20. Gergess, A. N., and N. Gerges. 2012. "Implication of Increased Live Loads on the Design of Precast, Prestressed Concrete AASHTO Girders." *PCI Journal* 57 (4): 78–95.

Notation

A_{nc} = cross-sectional area of prestressed concrete girder

b_v = web thickness

d_b = strand diameter

d_v = effective shear depth

e = eccentricity of prestressing tendons

f_c' = 28-day concrete compressive strength

f_{ci}' = concrete compressive strength at release

f_{pc} = compressive strength in concrete due to prestress

F = effective prestress force after long-term losses

I_{cg} = moment of inertia of precast concrete girder

l_t = transfer length of prestress force

L = design span length

M = moment

M_{cdl} = composite dead load moment

M_{cre} = cracking moment

M_{LL+I} = moment due to live load plus impact

M_{max} = factored moment due to externally applied loads

M_{ncdl} = noncomposite dead load moment

$(S_b)_c$ = bottom fiber composite section modulus

$(S_b)_{nc}$ = bottom fiber noncomposite section modulus

$(S_t)_c$ = top fiber composite section modulus

$(S_t)_{nc}$ = top fiber noncomposite section modulus

V_{ci} = shear capacity based on flexure-shear cracking

V_{cw} = shear capacity based on web-shear cracking

V_d = shear due to unfactored dead load

V_i = factored shear force due to externally applied loads

V_p = vertical component of prestress force (for draped strands)

w = distributed live load

Y_{bot} = distance from neutral axis of precast concrete girder to the bottom fiber

α = factor of increase in prestress force F

α_1 = factor of increase in number of prestressing strands

γ = factor of increase in prestress force F due to reductions in service load stress limits

$(\sigma_{all})_c$ = allowable concrete service load compressive stress

$(\sigma_{all})_t$ = allowable concrete service load tensile stress

About the authors

Antoine N. Gergess, PhD, PE, FASCE, is a professor of civil engineering at the University of Balamand in Lebanon, and a bridge specialist for Al-Meraikhi Industrial Complex in Abu Dhabi, United Arab Emirates.

Rajan Sen, PhD, PE, FASCE, FACI, is a professor of structural engineering at the University of South Florida in Tampa, Fla. He was previously with the Bridges Engineering Standards Division, Department of Transport, in London, U.K.

Abstract

Precast, prestressed concrete girders are often made continuous to support live loads and composite loads. Although American Association of State Highway and Transportation Officials (AASHTO) HL93 loads are adopted internationally, it is common practice in industrial zones where oversized/overweight trucks are the norm to design for greater live loads. The British Standards Institution's live loads can be as much as 50% higher than the HL93 loading and are therefore sometimes used in design.

This paper investigates the implications of increased live loads on the design of precast, prestressed concrete girders made continuous. The increase in positive moments due to increased live load is economically accommodated by increasing the prestressing force. However, this leads to overstress in the girder end zones over the intermediate supports. Recommendations for reducing these stresses by using debonded strands in excess of the 25% limit imposed by AASHTO are made by making the flanged section solid at its ends to increase the shear capacity locally.

Keywords

AASHTO, British Standards Institution, continuous, BSI, debonding, girder, HA, HB, HL 93, load.

Review policy

This paper was reviewed in accordance with the Precast/Prestressed Concrete Institute's peer-review process.

Reader comments

Please address any reader comments to journal@pci.org or Precast/Prestressed Concrete Institute, c/o *PCI Journal*, 200 W. Adams St., Suite 2100, Chicago, IL 60606.